Transactions of the **13th International Conference on Structural Mechanics in Reactor Technology** (SMiRT 13), Escola de Engenharia - Universidade Federal do Rio Grande do Sul, Porto Alegre, Brazil, August 13-18, 1995

Elevated temperature structural design guide for DFBR in Japan

Takakura, K.[1], Ueta, M.[2], Dozaki, K.[2], Wada, H.[3], Hirayama, H.[4], Hayashi, M.[5], Ozaki, H.[6], Ooka, Y.[7]

1) FBR Engineering Co., Ltd., Tokyo, Japan
2) The Japan Atomic Power Company, Tokyo, Japan
3) Mitsubshi Heavy Industries, Ltd., Kobe, Japan
4) Toshiba Corporation, Yokohama, Japan
5) Hitachi Ltd.., Hitachi, Japan
6) Fuji Electric Co., Ltd., Kawasaki, Japan
7) Kawasaki Heavy Industries, Ltd., Tokyo, Japan

ABSTRACT

The elevated temperature structural design guide (ETSDG)[1] for the Demonstration Fast Breeder Reactor (DFBR) in Japan, called DDS, is now under development based on ETSDG, which has been developed by Power Reactor and Nuclear Fuel Development Corporation (PNC) as the design standard for class 1 components of prototype fast breeder reactor "Monju". The Japan Atomic Power Company (JAPC) has been conducting the program to develop DDS in cooperation with PNC and Central Research Institute of Electric Power Industry (CRIEPI) and a number of FBR fabricators. DFBR in Japan is planned to apply new materials and new structural concepts, and therefore DDS should cover these new items.

This paper describes the recent status of the development of DDS focusing on the following topics.

1. Limits to accumulated inelastic strain (thermal ratchetting strain)
2. Elastic follow-up parameter (peak stress intensity)
3. Strength properties of new materials (316FR steel and mod.9Cr-1Mo steel)

1. INTRODUCTION

Improvements of structural materials and design evaluation methods contribute to assure cost reduction and high performance of liquid metal fast breeder reactor consistent with excellent reliability. JAPC has been conducting the program to develop the elevated temperature structural design guide for DFBR (DDS) in Japan in cooperation with PNC and CRIEPI.

DDS is based on ETSDG and modified to reflect structural and material features of DFBR, incorporating results of latest R&D. The preliminary draft of DDS has been prepared for elevated temperature class 1 components. This paper describes the recent status of the studies to develop DDS.

2. STUDY ITEMS TO DEVELOP DDS

(1) Limits to accumulated inelastic strain

Steep temperature gradient is caused and therefore large thermal stress may be generated in axial direction in the vicinity of sodium free surface of primary vessels of DFBR, due to the difference in thermal conductibility of liquid sodium from that of cover gas.

Since DFBR has no over-flow system in the primary circuit, free surfaces of liquid sodium in primary vessels and therefore thermal stress distributions in vessel walls move up and down cyclically during startup and shutdown.

It has been shown by the experiments that cyclic movement of severe thermal stress distribution may cause several types of thermal ratchetting. respectively.

(2) Limits to creep-fatigue damage

Results of not a few structural model tests has shown that the conventional method employed in ETSDG to evaluate creep-fatigue damage has too large safety margin.[2] The conservatism may be attributed to over-estimation of initial stress during stress relaxation and elastic follow-up parameter. ETSDG assumes that creep relaxation starts with the maximum stress in the cycle. However, initial stress of actual stress relaxation, for example during hold after hot shock, is often considerably smaller than the maximum. Therefore, ETSDG gives much conservative estimation of creep damage based on time consuming rule. DDS will introduce interim-hold concept[3] as shown in Fig. 1. In case that stress relaxation starts with considerably lower stress than the maximum, one extreme state to estimate strain range in the cycle may be hot steady state, and calculated relaxation curve based on interim-hold concept would be rationalized compared with the one based on ETSDG. The validity of interim-hold concept has been shown by creep-fatigue tests with holds at various points using SUS304 specimen[4].

Elastic follow-up intensifies strain concentration at a structural discontinuity. ETSDG applies a value of q=3 to an elastic follow-up parameter for both plastic and creep behavior, and results of inelastic analyses and model tests has revealed the conservatism of q=3. Since the value of q=3 would be much conservative in actual conditions encountered in design. Recent study on elastic follow-up parameter is described following section(3.2).

(3) Strain range of Weldment

It was the policy in the "Monju" design that the weldment should be kept sufficient distance from high stress regions such as the vicinity of sodium surface, so the special evaluation method of weldment strength was not required. Reactor vessel in DFBR has larger diameters, so it is not practical to fabricate it by integrally forging as applied to "Monju". Therefore, DFBR reactor vessel will have longitudinal weldments where high stresses may be caused due to steep temperature gradient in the vicinity of sodium surface.

DDS assumes smoothed weldment to be a kind of global discontinuity, and strain concentration factor at weldment could be expressed as the product of that of smoothed weldment and that due to local discontinuity. The strain concentration factor due to smoothed weldment could be calculated by equation (1)[5] as the case with that of base metal region with global discontinuity except introducing elastic follow-up intensification factor and correction factor to shakedown limit

$$K_e = \left[1 + (f_w \cdot q - 1) \cdot \left(1 - \gamma_y \cdot \frac{\overline{3Sm}}{\Delta\sigma_{el}} \right) \right] \quad \cdots\cdots (1)$$

where

Ke' : strain concentration factor due to elastic follow-up
$\Delta\sigma$el : elastically calculated stress range
qn : elastic follow-up parameter to primary plus secondary stress
γy : correction factor to the shakedown limit
fw : elastic follow-up intensification factor
$\overline{3Sm}$: shakedown limit

The validity of the evaluation method of weldment strength has been verified as shown in Fig.2 by creep-fatigue tests using SUS304-SUS308 welded joint specimen[6].

(4) Prevention of buckling

Since the ratio of diameter to axial length of the reactor vessel would be about 0.7, shear buckling load of the vessel would be comparable to bending buckling load. Therefore, DDS should provide evaluation method of buckling strength of a vessel subjected to not only axial compression and bending moment loads but also shear load. DDS will apply the interaction law of two types of buckling modes, that is, shear and bending modes, by 3 to 5 power law, based on the database of buckling test results of cylindrical models[7].

As for buckling strength under seismic loads, CRIEPI has been conducting the test program since 1987 under sponsorship of Ministry of International Trade and Industry. CRIEPI has proposed rationalized buckling criteria for cylinders under lateral seismic loads. This criteria applies response reduction factor, which considers reduction of seismic responses due to nonlinear load-displacement behaviors of vessels[8]. DDS would incorporate this concept with appropriate conservatism.

DDS would also provide the evaluation method of buckling strength of a cylinder with openings under a lateral load, which will use an expression of the buckling strength of a cylinder without openings multiplied by strength reduction factor considering openings.

(5)Design criteria for top entry piping

In "Monju", thermal expansion of a pipe is absorbed by deformation of the piping system with a number of elbows, on the other hand DFBR would apply the top-entry piping system, which comprises one horizontal pipe, two elbows and two vertical pipes connected to deck seal pipes with Y-shaped pieces, as shown in Fig.3.

a.Thermal expansion of a horizontal pipe is absorbed by bending deformation of two vertical pipes and two deck seals. Prevention of displacement-controlled buckling of vertical pipes is one of the critical issue in structural design.

b.Two elbows are subjected to nearly displacement-controlled bending load by thermal expansion. Assessment of progressive inelastic strain accumulation and creep-fatigue damage by large elastic follow-up is another critical issue in structural design.

c.Seismic loads are superimposed on thermal expansion loads. Endurable load of a top-entry piping under both thermal expansion and seismic loads should be evaluated.

It is a critical issue of piping design how to prevent thermal buckling of vertical pipes subjected to lateral displacement. Displacement-controlled buckling tests is performed using straight pipe models of 316FR. The test results have shown that test models would gradually collapse more than full plastic moment of cylinder and the start point of local buckling could be determined by bending strain near the fixed end. The critical deformation corresponding to the start point of buckling can be defined as the point where bending strain would begin to increase accelerativ ely.

The test results have shown that the critical rotation angle depends only on the ratio of pipe radius to wall thickness as shown in Fig.11 and independent of pipe length[5]. Evaluation method for displacement-controlled buckling of a straight pipe is proposed based on the test results as follows.

$$\theta_{cr} = 0.003 + 0.15 \cdot t/R \quad \ldots\ldots (10)$$

, where θ cr is critical rotation angle of vertical straight pipe, t is pipe thickness and R is radius of pipe. Above equation can be applied to Do/t<100. DDS provides this equation. Dynamic test was carried out to study deformation behavior of a inverted U-

shaped piping system subjected to seismic load superimposed thermal expansion load. The test result has shown that the maximum load under thermal expansion would be around the same value as that without thermal expansion[5].

(6) Strength and properties of new materials

Advanced 316 stainless steel (316FR) will be applied as a structural material of class 1 components of DFBR, because 316FR has excellent strength at elevated temperatures. Creep strength of 316FR at 600℃ is equivalent to that of SUS304 at 550℃.

Table 1 lists the chemical composition of 316FR[13]. 316FR has much lowered carbon content to prevent creep ductility from decreasing due to precipitation of carbides during long term exposure to elevated temperature environment, and 316FR has medium nitrogen added to improve strength at elevated temperatures.

Once-through type steam generator (SG) would be applied to DFBR for economical advantages. Tube material of this type SG should have enough strength at elevated temperature, high corrosion resistance to hot and wet environment, and good fabricability for coiling and welding. It has been revealed that the best candidate material to meet those requirements is modified 9Cr-1Mo steel, which has additional contents of V,Nb and N to conventional 9Cr-1Mo steel and has been widely used in thermal power plants. JAPC has been conducting material test program to prepare reliable draft of material strength standard of 316FR and modified 9Cr-1Mo steel.

3. RECENT STUDY ON DDS

3.1 Limits to accumulated inelastic strain

(1) Classification of inelastic strain

DDS restricts accumulated positive inelastic principal strain as follows.

Averaged strain through the thickness.....; 1%

Equivalent linear distributed strain through the thickness ...; 2%

In DDS, inelastic strain is expressed as the sum of the following strain components.

ε EC ; enhanced creep strain which would be caused under by core stress

ε R ; ratchetting strain

ε EF ; elastic follow-up strain.

Fig.5 shows the evaluation flow about the limitation of accumulated inelastic strain in DDS. Among those inelastic strain, ratchetting strain is explained following section.

(2) Ratchetting strain

In DDS, ratchetting strain classified by following three kinds of ratchetting strain.

$$\varepsilon R = \varepsilon R1 + (\varepsilon R2 \text{ or } \varepsilon R3) \quad \ldots\ldots (2)$$

ε R1 ; Bree type ratchetting strain

ε R2 ; Thermal ratchetting strain in the vicinity of free surface level

ε R3 ; Ratchetting strain by secondary hoop membrane stress (structural portion with no effect of axially moving of sodium surface)

(3) Thermal ratchetting strain in the vicinity of free surface level

Steep axial temperature gradient on the vessel walls near sodium surfaces may causes large thermal membrane stress beyond yield stress. When the axial temperature distribution through the wall travels cyclically in axial direction of a vessel, progressive radial deformation of the vessel might occur even though it is free from primary stress. JAPC have studied this type of ratchetting by conducting cylindrical model tests and FEM analyses, and has proposed a following predictive equation.

Basic prediction equation[9]

As for the simplest shapes of a temperature distribution, the step change and linear change , the following prediction equation of plastic ratchetting strain has been proposed by assuming the elastic-perfectly-plastic material and the long moving distance of temperature distribution.

$$\Delta \varepsilon_R = 2(\sigma_m - \sigma_y)/E \quad \cdots\cdots (3)$$

, where $\Delta \varepsilon$ R, σ m, σ y and E are the increment of ratchetting strain, the elastically-obtained hoop-membrane stress, the yield stress of material and the Young's modulus, respectively. FE analyses show that the increment of the ratchetting strain mainly correlates with σ m , and the prediction by equation(1) is conservative for the most cases. But the correlation with the axial bending stress σ z is found at the low stress level where axial bending stress σ b is found at the low stress level where σ m is at around the yield stress σ y, and some results are unconservative.

Consideration of bending stress[9]

A new prediction equation which considers the contribution of σ b in addition to that of σ m is proposed as follows.

$$\Delta \varepsilon_R = 2(\sigma_m - \bar{\sigma}_y)/E \quad \cdots\cdots (4)$$

, where $\bar{\sigma}_y = \bar{\sigma}_y(\sigma_m, \sigma_b)$ is the equivalent yield stress which can be determined from both σ m and σ b. The equivalent yield stress is concretely defined as the hoop membrane stress when all points through the wall thickness are in plastic state.

$$\int_{-1/2}^{1/2} \sigma_\theta(x)dx = \frac{\sqrt{3}}{2}\cdot\frac{\Delta\varepsilon_2}{\Delta\varepsilon_1}\cdot\ln\left(\frac{\sqrt{\Delta\varepsilon_1^2+3\Delta\varepsilon_2^2}+\Delta\varepsilon_1}{\sqrt{\Delta\varepsilon_1^2+3\Delta\varepsilon_2^2}-\Delta\varepsilon_1}\right)\cdot\sigma_y \quad \cdots\cdots (5)$$

The effect of axial bending loading is schematically shown in Fig.6. When there is no axial bending, hoop-membrane stress-strain curve shows the uni-axial stress-strain curve of base metal with the yield stress σ y. When there is axial bending, on the other hand, hoop-membrane stress-strain curve shows lowered yield stress $\bar{\sigma}_y$.

Consideration of primary stress[9]

A reactor vessel of FBR is subjected to a small amount of primary tensile stress due to dead weight in addition to the thermal stress. To consider this primary stress, the equation is improved by following procedure. In this case, axial equilibrium equation is as follows.

$$\int_{-1/2}^{1/2} \sigma_z(x)dx = \frac{3}{2}\cdot\sigma_y\cdot\left[\sqrt{3X^2+3(2P+1)\cdot\frac{1}{A}+3(P^2+P+1)\cdot\frac{1}{A^2}}\right]_{-1/2}^{1/2} = \sigma_p \quad \cdots\cdots (6)$$

, where $A=\Delta\varepsilon_1/\Delta\varepsilon_2$, $P=\Delta\varepsilon_0/\Delta\varepsilon_2$ and ε_0 is axial membrane strain increment. If the value of A is assumed, the value of P is numerically obtained from equation(6). The modified hoop membrane stress is obtained from the following equation by using the values of A and P.

$$\bar{\sigma}_y = \int_{-1/2}^{1/2}\sigma_\theta(x)dx = \sigma_y\cdot\int_{-1/2}^{1/2}\frac{\{(2+P)/A+x\}dx}{\sqrt{3X^2+3(2P+1)\cdot\frac{1}{A}+3(P^2+P+1)\cdot\frac{1}{A^2}}} \quad \cdots\cdots (7)$$

The ratchetting strain increment under the primary stress can be obtained by substituting the equation(7) to the equation(4). Ratchetting criteria is showed in Fig.7, this figure shows that criteria is narrowed down by primary stress. In case of $(|\sigma m|-\sigma p)/\sigma y$ for horizontal axis instead of σm, in actual primary stress level($\sigma p<0.2\sigma y$), non ratchetting region is bounded on null primary stress line.

Consideration of moving distance[10]

The decrease of ratchetting strain increment under the short travel of temperature distribution was confirmed by inelastic analyses and experiments. Figure 8 shows the mechanism of the effect of moving distance. In the case of long travel of temperature distribution, the ratchetting deformation is shown as the solid line in this figure, and residual stress does not exist in the flat part of deformation at the center of traveling. Therefore, the ratchetting strain increment at this part is constant for every cycle.

On the other hand, in the case of short travel, the deformation at the center of traveling becomes small due to the constraint by the regions ab and cd which are not subject to the traveling. As a result, the residual stress occurs in the opposite direction to the progress of ratchetting deformation, and the ratchetting strain increment at the second cycle becomes smaller than that at the first cycle by the effect of this residual stress. After a number of cycles, the ratchetting strain increment becomes smaller, and the residual stress becomes larger.

It is necessary to predict the change of residual stress in order to predict the ratchetting strain increment of short travel. Modified prediction equation is proposed by assuming the short travel of hot-spot-shaped temperature distribution.

As for the case in which the stresses at boundaries of traveling are below the yield stress, the prediction equation is proposed by assuming that the ratchetting strain increment decrease cycle by cycle with equal ratio by residual stress effect.

$$\Delta \varepsilon_R = (\Psi+1)\,\gamma_0^{N-1}(\sigma_m-\sigma_y)/E \qquad \cdots\cdots (8)$$

, where ψ、γ_0 are function of moving distance, σ_m is range of elastic-hoop-membrane stress, σy is a yield stress, E is Young's modulus, and N is number of cycle.

On the other hand, as for the case in which the stresses at boundaries of traveling reach the yield stress, the following prediction equation is proposed by assuming that the ratchetting strain increment becomes constant after either stress of start point or end point of traveling reaches the yield stress.

$$\Delta \varepsilon_R = (\Psi+1)\,\gamma_0^{N_s-1}(\sigma_m-\sigma_y)/E \qquad \cdots\cdots (9)$$

, where Ns is number of cycle when the plastic yielding occurs at either boundary of traveling.

Without residual stress, ratchetting strain increment per cycle can be calculated by the difference between the maximum hoop membrane stress and the modified yield stress divided by Young's modulus. Where the modified yield stress is calculated taking the fact into account that axial bending stress enhances the ratchetting strain.

If the travel of temperature distribution is short, residual stress field develops and strain increment decreases cycle by cycle. The predictive equation includes a factor on this effect, which depends on travel distance and cycle number. The equation can give reasonably conservative prediction of ratchetting strains compared with FE analyses as shown in Fig.9.

3.2 Elastic follow-up parameter

In creep fatigue dame estimation, inelastic strain range can be calculated by multiplication of gross strain concentration due to global structural discontinuity and

local strain concentration at local structural discontinuity.

Therefore elastic follow-up parameter should be taken into consideration to both strain concentration behaviors. DDS provides the elastic follow-up parameter qn to the primary plus secondary stress to the global structural discontinuity and qp as the elastic follow-up parameter related to the peak stress intensity at local structural discontinuity[14]. The qn is used to calculate the inelastic strain range in creep-fatigue damage estimation and the qp is to calculate creep damage associated with stress relaxation of the peak stress intensity. DDS allows to use qn=3 for general structure and qn=2 for special structure such as stepped cylinder with axial temperature distribution[5]. When the stress relaxation accompanied with elastic follow-up, stress relaxes slowly and the creep damage should be larger than in the case without elastic follow-up. The elastic follow-up parameter qp related to the peak stress intensity is used in the stress relaxation calculation.

DDS provides following equation for elastic follow-up parameter qp,

$$qp = K \cdot qn \ , \qquad \cdots\cdots\cdots (10)$$

where

qp : elastic follow-up parameter for peak stress intensity
qn : elastic follow-up parameter for primary plus secondary stress
K : elastic stress concentration factor.

This equation is based on the analogy of peak stress intensity consideration, that is estimated by nominal stress multiplied by amplitude factor Neuber's rule including elastic stress concentration factor K for nominal stress distribution. Verification of above equation is confirmed by thermal transient test using cylindrical shell with notch model and stepped cylinder model, as shown in Fig.10. From Figure 10 ,it is shown that qp is less than Kqn .

3.3 Strength and properties of new materials

A research committee has been organized since 1985 in the Japan Welding Engineering Society under sponsorship of JAPC. The aims of this committee are as follows.

a. Confirmation of the applicability of 316FR and modified 9Cr-1Mo steel to DFBR structure
b. Evaluation of strength properties of the two materials
c. Optimization of the specification of the two materials and their welding materials
d. Technical advice for standardization of the two materials

A Test program of 316FR base metal and welding material has started in FY1991. Some test results of plate and forging material have been obtained. Creep rupture strength of 316FR is excellent, compared with SUS304 and conventional SUS316, especially under long term exposure to high temperature environment as shown in Fig.11[11]. Low cycle fatigue strength of 316FR would be the same level as that of SUS304 and conventional SUS316. Test program will continue until FY1998.

As for welding material, 17 charges of TIG wires for 316FR were fabricated and have been tested. 17 charges are composed of following three types,

- type 316 with low carbon contents and medium nitrogen added
- type 16-8-2
- the type with chemical composition between the former two

All charges shows good weldability. Remarkable difference is not seen in tensile strength at room temperature and 600°C. A series of tests on the welding materials is ongoing, namely creep rupture tests at 600°C and Charpy impact tests after 1000hr ,3000hr and 10000hr aging at 550, 600 and 650°C, and fatigue and creep-fatigue tests at

600°C. The addition of Nb and Ti tends to increase relatively short term creep strength, but this effect might diminish in long term range. Long term exposure to elevated temperature tends to decrease Charpy impact values.This effect seems to be small in case of low Cr content and low delta-ferrite materials.

A test program of modified 9Cr-1Mo steel has started in FY1985. It has been already confirmed that modified 9Cr-1Mo steel would be applicable and feasible as a material of steam generators of DFBR. Creep strength of base metal of modified 9Cr-1Mo steel can be estimated using the PNC's equation, and that of weldment can be estimated by introducing strength reduction factor. Forging material with 550mm thickness has almost the same creep rupture strength as plate material with 25mm thickness does.

It has been shown that modified 9Cr-1Mo steel has rather high fatigue strength at room temperature and 300°C, compared with carbon steel and so on, therefore the design fatigue curve superior to others could be specified for modified 9Cr-1Mo steel, meanwhile ASME CODE applies the same design fatigue curves for carbon steel and low alloy steel including modified 9Cr-1Mo steel. For example, comparison of creep rupture strength of 9Cr type steels with 2.25Cr-1Mo and SUS304 is shown in Fig.12.[12]

JAPC has been conducting a series of tests of 316FR and modified 9Cr-1Mo steel focusing on long-term creep tests over 10000hr, fatigue tests of low strain rates or low strain range, and creep-fatigue tests of low strain range with long hold time. The test results would be compiled as database for standardization of these materials.

4.CONCLUDING REMARKS

We have introduced the current status of DDS, the elevated temperature structural design guide for the Demonstration Fast Breeder Reactor in Japan. DDS will introduce improved evaluation methods of accumulated inelastic strain, creep-fatigue damage of base metal and weldment, buckling, and design method for top-entry piping system and so on. DDS will also provide material strength standard of 316FR and modified 9Cr-1Mo steel. We will further elaborate to establish DDS reflecting the results of latest R&D in cooperation with PNC and CRIEPI.

ACKNOWLEDGEMENTS

Activities in this study has been performed as a part of joint research and development projects for the DFBR under the sponsorship of nine Japanese electric power companies, Electric Power Development Co.,Ltd. and the Japan Atomic Power Company.

The authors would like to express their sincere gratitude to researchers and engineers of PNC, CRIEPI for the fruitful comments and discussion.

REFERENCES

[1]Iida,K.et al.;Construction Codes Developed for Prototype FBR Monju,Nucl.Engrg.Des.,98,(1987),pp.283-288.

[2]Watashi,K.et al.;Creep-Fatigue test of thick-walled vessel under thermal transient loadings,Nucl.Engrg.Des., 116,(1989),pp.423-441.

[3]Nagata,T.and Imazu,A.,Advancement in Elevated Temperature Structural Design Guide for FBR,Proceedings of Post Conference Seminar of 10th SMiRT on

Construction Codes and Engineering Mechanics,2A,pp.1-35.
[4]Kagawa,H.et al.;Creep-Fatigue Strength of SUS304 Welded Joints at 550℃ and the Evaluation on the Basis of Strain Concentration,J.of the Society of Materials Science,vol.39,No.440,pp.503-508.
[5]Takakura,K.et al.;Improvement of Elevated Temperature Structural Design Guide for DFBR in Japan,SMiRT-12,E03/1.
[6]Komine,R.et al.;Effect of Strain Hold Position on Creep-Fatigue Life of SUS304,Proc.of 1991 Fall Meeting of AESJ,F6.
[7]Akiyama,H.et al.;Buckling Strength Evaluation of FBR Main Vessels under Lateral Seismic Loads,SMiRT-11,E10/1.
[8]Akiyama,H.et al.;Outline of the Seismic Buckling Design Guideline of FBR-A Tentative Draft-,SMiRT-11,E09/1.
[9]Wada,H.et al.;Proposal of a new estimation method of thermal ratchetting behavior of FBR components,SMiRT-11 Seminar11,August(1991).
[10]Kitade,S.et al.;Proposal of an Estimation Method of Thermal Ratchetting of FBR Components Subjected to Short Travel of Temperature Distribution,SMiRT-11Seminar11,(1991).
[11]Nakazawa et al.;J.of Iron Steel Inst.Japan,75-12(1989)2234.
[12]Asada,Y.et al.;Research and Development on 9Cr-Steel for Steam Generator of DFBR,SMiRT-11 Vol.L,August(1991).
[13]Ueta,M.et al.;Current Status of Structural Design Guide for DFBR in Japan,SMiRT-12,Seminar No.11.
[14]Hirayama,H.et al.;Creep-Fatigue Evaluation Rules in Design Guide for DFBR in Japan,ASME PVP,(1995)to be published.

Table.1 Chemical composition range of 316FR stainless steel

Material	Chemical composition (wt%)												
	C	Si	Mn	P	S	Ni	Cr	Mo	N	Al	Nb	B	Co
316FR	≤ 0.020	≤ 1.00	≤ 2.00	0.020 ~ 0.040	≤ 0.030	10.00 ~ 14.00	16.00 ~ 18.00	2.00 ~ 3.00	0.06 ~ 0.12	≤ 0.05	—	≤ 0.001	≤ 0.25

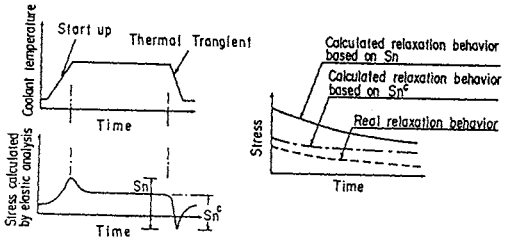

Fig.1 Interim-hold concept on initial stress in creep damage evaluation[13]

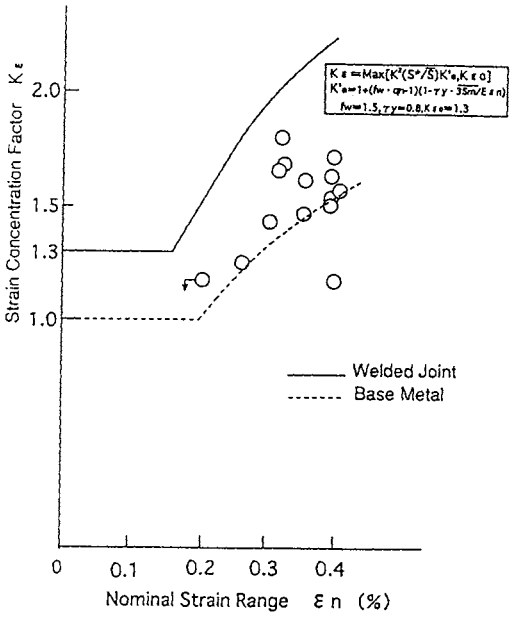

Fig.2 Strain Concentration factor of welded joint of SUS304 stainless steel[13]

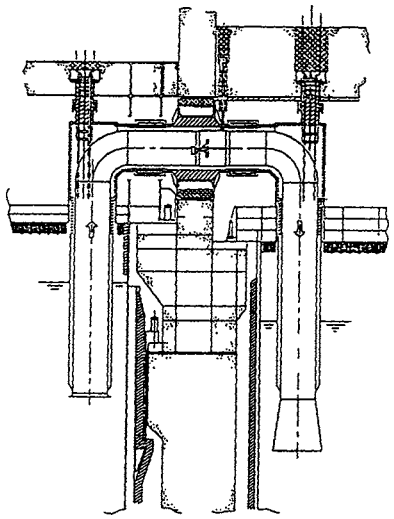

Fig.3 Top-Entry Piping system[13]

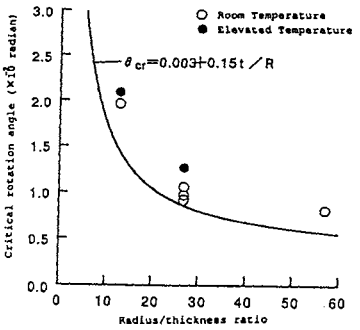

Fig.4 Dependency of critical rotation angle on radius/thickness ratio[13]

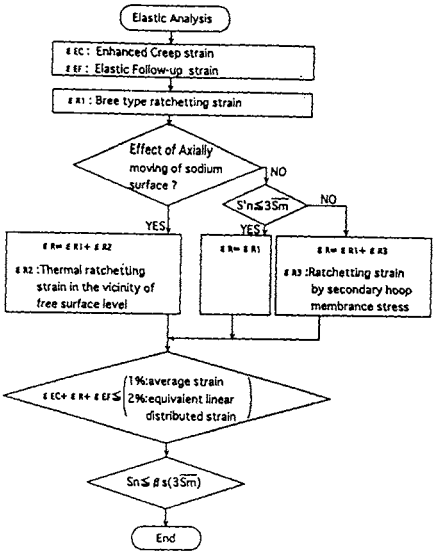

Fig.5 Evaluation flow about the limitaion of accumulated inelastic strain

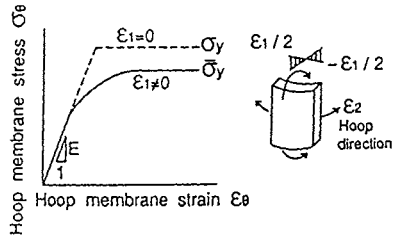

Fig.6 Hoop membrane stress-strain behavior[9]

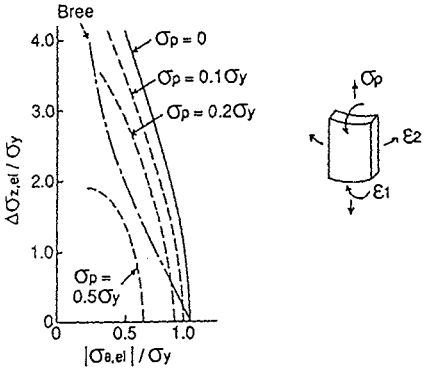

Fig.7 Non ratchetting region considering primary stress[9]

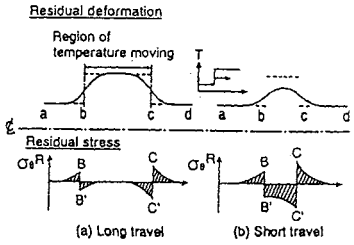

Fig.8 Mechanism of the effect of moving distance[10]

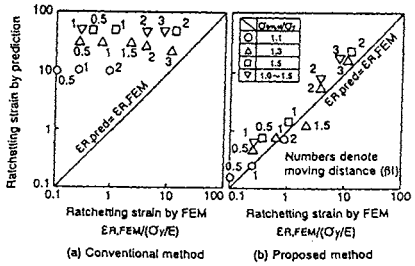

Fig.9 Comparison of predicted ratchetting strains with FE analyses[10]

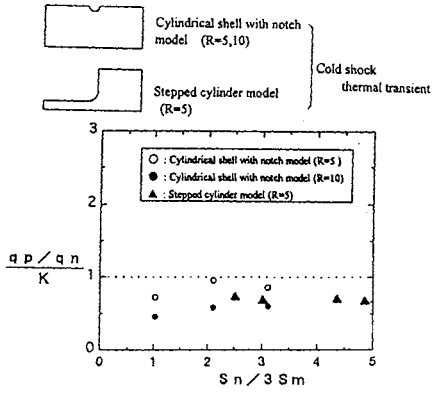

Fig.10 Thermal transient test using cylindrical shell model and stepped cylinder model

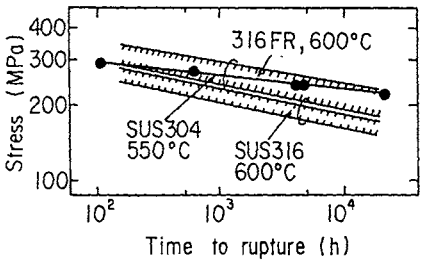

Fig.11 Comparison of creep rupture strength for SUS304 steel and SUS316 steel and 316FR steel [13]

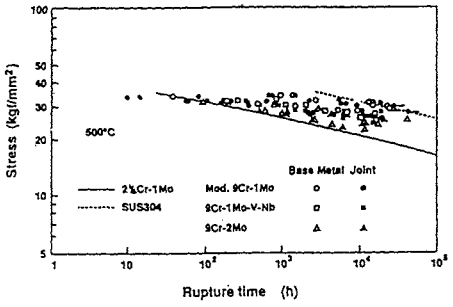

Fig.12 Comparison of creep rupture strength for 9Cr type steels with those for 2.25Cr-1Mo steel and SUS304 steel at 500°C[12]